IEEE Access
Multidisciplinary | Rapid Review | Open Access Journal

Received 15 December 2022, accepted 18 January 2023, date of publication 30 January 2023, date of current version 2 February 2023.

Digital Object Identifier 10.1109/ACCESS.2023.3240678

RESEARCH ARTICLE

A Novel Improved Manta Ray Foraging Optimization Approach for Mitigating Power System Congestion in Transmission Network

KAUSHIK PAUL[1], PAMPA SINHA[2], YASSINE BOUTERAA[3,4], PAWEŁ SKRUCH[5], (Senior Member, IEEE), AND SALEH MOBAYEN[6], (Senior Member, IEEE)

[1]Department of Electrical Engineering, BIT Sindri, Dhanbad 828123, India
[2]School of Electrical Engineering, KIIT University, Bhubaneswar 751024, India
[3]College of Computer Engineering and Sciences, Prince Sattam bin Abdulaziz University, Al-Kharj 11942, Saudi Arabia
[4]Control and Energy Management Laboratory (CEM Lab), Ecole Nationale d Ingenieurs de Sfax (ENIS) & Institut Superieur de Biotechnologie de Sfax (ISBS), University of Sfax, Sfax 3038, Tunisia
[5]Department of Automatic Control and Robotics, AGH University of Science and Technology, 30-059 Kraków, Poland
[6]Graduate School of Intelligent Data Science, National Yunlin University of Science and Technology, Douliou, Yunlin 640301, Taiwan

Corresponding authors: Kaushik Paul (kaushik.ee@bitsindri.ac.in) and Saleh Mobayen (mobayens@yuntech.edu.tw)

ABSTRACT This research manuscript proposes an Improved Manta Ray Foraging Optimization (IMRFO) algorithm for the power system congestion cost problem. The goal of the proposed Congestion Management (CM) strategy is twofold: firstly, the Generator Sensitivity Factors (GSF) is determined to select and involve the most influential power system generators that will reschedule their real power to alleviate the excess power flow in congested transmission lines. Secondly, the IMRFO has been developed and applied to attain the minimum possible congestion cost. The IMRFO has been formulated with the inclusion of correction factors in the exploration and exploitation phases to improve the coordination between these phases. The effectiveness of IMRFO has been measured considering its effective performance on the 23 conventional benchmark functions. 39 bus New England and IEEE-118 bus test system has been utilized to authenticate the effectiveness of the CM approach with the application of IMRFO. The outcomes highlight that the congestion cost achieved with IMRFO has been reduced by, of 16.08%, 13.73%, 11.78%, and 4.48 % for the 39-bus system and 14.84%, 12.97%, 9.63%, and 6.85% for 118 bus system when compared to the Bacteria Forge Optimization (BFO), Grey Wolf Optimization (GWO), Sine-Cosine Algorithm (SCA), and Original MRFO. The results gained with the implementation of IMRFO on the CM problem portrays appreciable minimization in the congestion cost, enhancement in the system voltage and losses, generates better convergence profile and computational time when contrasted with the recent optimization methods.

INDEX TERMS Manta ray forge optimization, meta-heuristic technique, optimal power flow, optimization, power rescheduling, sensitivity analysis.

I. INTRODUCTION

The deregulated mode of power system operations has given rise to intense competition among its market players. Each player in the electricity market tries to achieve maximum profit based on the power transactions which has necessitates the utilization transmission corridors to its full capacity for power transmission. In such scenarios, the power generation must match the load demand to maintain an optimal power system operation. Any mismatch between the generation and load may lead to the violation the transfer limits which may give rise to a congested power system network. Thus, it becomes the major responsibility of the Independent System Operator (ISO) to maintain the reliability and stability of the power system network by reliving the congestion.

The associate editor coordinating the review of this manuscript and approving it for publication was Ahmed F. Zobaa.

The task of managing the congestion has been an integral issue with heightened competition in the electricity market. The proliferation of auxiliary facilities and the consolidation of networks result in the emergence of a competitive spirit among the market players. Maintaining the operation of the transmission lines below its thermal limit with the implementation of the optimal power generation is an effective approach to manage the congestion. The congestion in the power system network can significantly affect the technical and financial component of the power system and is one of the primary issues faced by the ISO. This enables the power market players to utilize the transmission network to its maximum limits. This scenario necessitates the adaptation of effective CM strategies.

There are several Congestion Management (CM) strategies that have been implemented by the by the power system operators to maintain an optimal power system operation. In [1], Hobbie et al. planned a model parameterization method for analysing the effectiveness of the renewable energy system's behaviour towards mitigation of the congestion in the power system grid. Chakravarthi et al. in their research developed a controller based model for CM that can control the performance of Battery Energy Storage System (BESS) and can reschedule the generators based upon the actual signal received from the congested power system grid [2]. Sarwar et al. adopted the optimal placement of the Distribution Generation (DG) considering the locational marginal pricing scheme to manage the line flows. Hybrid swarm optimization techniques has been implemented in their work for the optimal placement [3]. In another research, Roustaei et al. managed congestion with the transmission switching application to enhance the system stability by controlling the active and reactive power measurements of the power system transmission lines [4]. Prajapati and Mahajan formulated a demand response based CM with the implementation of the Monte Carlo simulation to control the unpredicted nature of the power delivery by the renewable energy sources [5]. Jasmine et al. implemented the FACTS devices to manage the congestion for the bilateral, and multi-lateral transactions [6]. Deepti et al. formulated a CM approach which aim towards maintaining the power purchase agreements while utilizing the reserved capacity in the electricity markets. The CM has been performed with the implementation of the GR approach with the security constrained optimal power flow [7]. In general, the ISO adopt the Generator Rescheduling (GR) among the various CM strategy because the implementation of the GR doesn't require significant modifications in the power system network topology and is considered as the most economical CM strategy.

A. LITERATURE SURVEY

The CM strategies perform an essential role in deregulated framework of power system to assure normal power system operations. Details of CM methodologies based on the in several types of electricity market structures can be found in [8]. Wang et al. in their research introduced the effective management of the storage devices in muti-area power system context to manage the congestion and frequency through a virtual storage plant. In their research a distributed optimization approach has been adopted for the coordination of the virtual storage plants and mitigating congestion in the tie line power flow while providing frequency support [9]. Zhou et al. proposed a CM strategy that consider the determination of the congestion cost sharing in the electricity market, and the other is the procuring of the services in the ancillary service market that aim towards the congestion cost minimization. They incorporated the cost and benefit constraints in the CM model to diminish the economic loss that are subjected to the grid and consumers [10]. Faheem et al. implemented a game theoretic approach to mitigate congestion considering the penetration of the electric vehicles in the microgrid. The optimal charging and discharging procedures of the electric vehicles are conducted to mitigate the situation of congestion while minimizing the change in the power injected by the electric vehicles [11]. Shen and Wu, proposed a dynamic tariff approach for day-ahead CM considering the uncertainty in the dynamic tariff framework. Their work illustrated that their proposed dynamic tariff framework method can handle the congestion adeptly under the uncertain condition while considering the SO forecast errors [12]. Voswinkel et al. proposed Shapley value game theoretic approach to share an over-all surplus produced by the partnership of the market established on their marginal assistances to their participation in the electricity market. They utilized this approach to share the CM costs between the power system grid essentials depending on individual supports to the aggregated CM costs [13].

The Generator Rescheduling (GR) technique, as well as the utilisation of Optimal Power Flow (OPF), have traditionally been considered very competent methods for CM. In [14] an OPF based approach considering the GR technique has been developed to control the transmission of excess power flowing through the lines. In another research, Srivastava and Yadav proposed a hybrid lion and moth search technique for the optimal GR of real power to alleviate congestion while maintaining the stability limits [15]. In [16], Yesuratnam and Thukaram also used the GR technique for CM. The generators, whose power need to be rescheduled have been considered in accordance to the Relative Electrical Distance (RED). Azab et al. formulated a GR method with the inclusion of the renewable energy sources. The objective of their research work aimed towards minimizing and maximizing the rescheduling cost and power system reliability respectively for CM [17]. In [18] Kumar and Shekhar portrayed a comparative study based on GR to minimize the effect of congestion considering best location for the Unified Power Flow Controller (UPFC). Dutta and Singh in their research, rescheduled the generators based on the sensitivity analysis and Particle Swarm Optimization (PSO) has been implemented to attain congestion cost minimization. [19].

Hazra et al. used a combination of GR and energy consumption on the load side to lighten the congestion in the network [20]. Agrawal et al. developed a CM model based on the hybrid neural network with the application of GR for the spot electricity market model [21]. In [22], Verma and Mukherjee proposed a Firefly Algorithm (FFA) to curtail the rescheduling cost involved in the handling the congestion in the power transfer corridors. Pandya et al. managed congestion by selecting the generators taking part in the rescheduling approach for CM based on the power sensitivity parameters. The output of the generators are adjusted considering the generator sensitivity values, and the rescheduling cost is calculated correspondingly [23]. In another research for CM, the combination of a generator rescheduling strategy and demand response has been implemented to decrease line overloading while keeping congestion costs to a minimum [24]. Raja et al. in their research performed CM using Nelder Mead -Grey Wolf Optimization to reschedule the active power of the generators [25]. Deb et al. in their research have developed the Artificial Bee Colony (ABC) algorithm to optimally manage generators' power delivery for congestion alleviation [26].

The competitive energy market operations have prompted the development of efficient optimization algorithms that are very successful in addressing power system issues with precise and better outcomes. The power system researchers have used deterministic methodologies, which include the classical method of approaches, to analyse the optimum power production and dispatch issue. The optimal power system operations issues have been studied using a variety of traditional approaches such as nonlinear programming [27], quadratic programming [28], and mixed integer programming [29]. The application of these deterministic approaches are restricted to a number of model constraints, including correct application of differentiability and convexity [30]. In such scenarios the results delivered with these approaches are significantly impacted by the starting solution, which may have a potential tendency to get restricted into regions of local optima. In such situations, stochastic techniques are a more effective alternative in comparison to deterministic calculations since they circumvent the drawbacks introduced by the application of deterministic techniques. This scenario encourages the implementation of the heuristic and meta-heuristic techniques, since they are substantially more capable of delivering greater outcomes than deterministic procedures [31], [32]. Several researchers in their research studies have adopted such similar effective techniques to identify the appropriate solution for optimum power production in order to ensure sustainable power flow through transmission corridors. PSO [19], Gravitational Search Algorithm (GSA) [33] ABC [28], FFA [22], Flower Pollination Algorithm (FPA) [34], Cuckoo Search Algorithm (CSA) [35], and improved Crow Search Algorithm (CSA) [36] are some of such approaches implemented to supervise the optimal power system operations. Suitable assortment and adjustment of the control parameters related to the meta heuristic techniques has a substantial impact on the solution achieved with its application. Meta-heuristic techniques provide a realistic alternative for achieving optimum solution with less computing processes. The integral goal of this proposed work is to develop and adopt an appropriate optimization strategy for the CM issue that will have a substantial impact on the expected output for cost minimization.

In the year 2020, Zhao et al. developed a swarm-based optimization method mimicked from the framework of manta ray foraging behaviour and has been termed as Manta Ray Foraging Optimization (MRFO) [37]. Application of MRFO in engineering optimization problems have delivered appreciable outcomes. Abd Elaziz et al. implemented MRFO for multilevel threshold visual segmentation using fractional order calculus [38]. Ghosh et al. in their research work formulated an enhanced MRFO that overcomes the issue of feature selection [39]. Xu et al. implemented MRFO, for the optimization and analysis of a high-temperature proton exchange membrane fuel cell [40]. In [41], Hemeida et al. utilized MRFO to achieve the optimal position for the DGs in the consumer side to enhance the voltage profile. Fathy et al. suggested an optimal maximum power point tracker using MRFO [42].

It can be seen that conventional MRFO has delivered considerable outcomes related to engineering optimization problem but MRFO has the drawbacks of limited exploration and exploitation capability, declining population variety, and a propensity to slip into local optimum. These flaws are mostly the result of disparity in the algorithm's exploitation and exploration phases. Thus, to overcome these shortcomings, an Improved MRFO (IMRFO) has been formulated with the inclusion of the improvement factors that will maintain an effective coordination in the exploration and exploitation phases. Appropriate assortment and adjustment of the parameters and constraints related to the meta heuristic approaches has a substantial impact on the solution achieved with its application.

The contribution of the research work can be stated as:

(i) Formulation of a CM approach with the optimal management of real power from the most sensitive generators that are selected considering generators sensitivity factor.

(ii) An Improved MRFO (IMRFO) has been proposed to implement it as an effective optimization technique to minimize the congestion cost by optimally rescheduling the real power of the generators.

(iii) Potency of the IMRFO has been tested on the conventional benchmark functions and the effectiveness of IMRFO has been analysed with its application on 39-bus New England system and a higher power system network of 118 bus system for CM with optimal minimization of congestion cost.

(iv) Comparative analysis has been established to highlight the efficacy of the proposed CM approach by comparing the results delivered by IMRFO with the results obtained with optimization algorithms like Gradient method, Bacteria Forge Optimization (BFO), Grey Wolf Optimization (GWO), Sine-Cosine Algorithm (SCA), and Original MRFO.

TABLE 1. Unimodal benchmark functions representations.

Function	*Mathematical representation*	*Dimensions, Limits*
Sphere	$f_1(z)=\sum_{i=1}^{k} z_i^{\,2}$	*30, [−100, 100]*
Schwefel 2.22	$f_2(z)=\sum_{i=1}^{k}\lvert z_i\rvert+\Pi_{i=1}^{k}\lvert z_i\rvert$	*30, [−10, 10]*
Schwefel 1.2	$f_3(z)=\sum_{i=1}^{k}\left(\sum_{j=1}^{n} z_j\right)^2$	*30, [−100, 100]*
Schwefel 2.21	$f_4(z)=\max_i\{\lvert z_i\rvert,1\le i\le k\}$	*30, [−100, 100]*
Rosenbrock	$f_5(z)=\sum_{i=1}^{k-1}\left[100(z_{i+1}-z_i^2)^2+(z_i-1)^2\right]$	*30, [−30, 30]*
Step	$f_6(z)=\sum_{i=1}^{k}([z_i+0.5])^2$	*30, [−100, 100]*
Quartic	$f_7(z)=\sum_{i=1}^{k} iz_i^{\,4}+random(0,1)$	*30, [−1.28, 1.28]*

The organization of this manuscript has been portrayed as: Section II highlights the problem formulation, conventional Manta Ray forge Optimization algorithm has been described in Section III, Section IV portrays the Improved Manta ray Forge optimization algorithm for the CM and represents its performance analysis. Section V states the Results and discussion and Section VI states the conclusion of the research work.

II. PROBLEM FORMULATION

The generators within the power system framework have varying sensitivities towards the congested line power flow. The variation in the power flow within a congested transmission channel k joining the i^{th} and j^{th} buses due to the modulation in real power delivered by the g^{th} generator can be stated as the Generator Sensitivity Factor (GSF). This can be represented mathematically as follows:

$$GSF_g=\frac{\Delta P_{ij}}{\Delta P_{Gg}} \tag{1}$$

Here in Equation (1) ΔP_{ij} represents the variation in the real power flowing in the congested transmission channel between the i^{th} and j^{th} buses and ΔP_{G_g} is the g^{th} generator's real power output. ISO identifies the generators with the most deviated GSFs and engage those generators to involve in CM strategy.

The power flow associated with the congested line can be represented as:

$$P_{ij}=-V_i^2G_{ij}+V_iV_jG_{ij}\cos(\theta_i-\theta_j)+V_iV_jB_{ij}\sin(\theta_i-\theta_j) \tag{2}$$

Here in Equation (2), G_{ij} is the conductance and B_{ij} resembles the susceptance of the transmission channel, voltage magnitude is denoted by V_i and θ_i represents the phase angle. Neglecting the P-V coupling, Equation (1) can be represented as:

$$GSF_g=\frac{\partial P_{ij}}{\partial\theta_i}\cdot\frac{\partial\theta_i}{\partial P_{G_g}}+\frac{\partial P_{ij}}{\partial\theta_j}\cdot\frac{\partial\theta_j}{\partial P_{G_g}} \tag{3}$$

The first term corresponding to both of the two product component in Equation (3) can be found by differentiating Equation (2), which is represented as follows:

$$\frac{\partial P_{ij}}{\partial\theta_i}=-V_iV_jG_{ij}\sin(\theta_i-\theta_j)+V_iV_jB_{ij}\cos(\theta_i-\theta_j) \tag{4}$$

$$\frac{\partial P_{ij}}{\partial\theta_j}=+V_iV_jG_{ij}\sin(\theta_i-\theta_j)-V_iV_jB_{ij}\cos(\theta_i-\theta_j)=-\frac{\partial P_{ij}}{\partial\theta_i} \tag{5}$$

The real power injection at the h^{th} bus can be stated as:

$$P_h=P_{G_h}-P_{D_h} \tag{6}$$

Here in Equation (6), P_{D_h} represents the power demand at the load bus h and P_h can be represented as:

$$P_h=V_h\sum_{t=1}^{n}((G_{ht}\cos(\theta_h-\theta_t)+B_{ht}\sin(\theta_h-\theta_t))V_t)=V_h^2G_{hh}+V_h\sum_{\substack{t=1\\t\neq h}}^{n}\{(G_{ht}\cos(\theta_h-\theta_t)+B_{ht}\sin(\theta_h-\theta_t))V_t\} \tag{7}$$

Here n denoted the total number of buses.

Differentiating Equation (7), w.r.t. θ_h and θ_t can be represented as:

$$\frac{\partial P_h}{\partial\theta_t}=V_hV_t\{G_{ht}\sin(\theta_s-\theta_t)-B_{ht}\cos(\theta_s-\theta_t)\} \tag{8}$$

$$\frac{\partial P_h}{\partial\theta_h}=V_h\sum_{\substack{t=1\\t\neq h}}^{n}\{(-G_{ht}\sin(\theta_h-\theta_t)+B_{ht}\cos(\theta_h-\theta_t))V_t\} \tag{9}$$

The incremental changes in real power at system buses and voltage phase angles may be stated as:

$$[\Delta P]_{n\times1}=[H]_{n\times n}[\Delta\theta]_{n\times1} \tag{10}$$

TABLE 2. Multi-modal benchmark functions representations.

Function	*Mathematical representation*	*Dimensions, Limits*
Schwefel	$f_8(z)=\sum_{i=1}^{k}-z_i\ +sin(\sqrt{\lvert z_i\rvert})$	*30, [–500,50]*
Rastrigin	$f_9(z)=\sum_{i=1}^{k}[z_i^2-10\cos(2\Pi z_i)+10]$	*30,[−5.12, 5.12]*
Ackley	$f_{10}(z)=-20\exp\left(-0.2\sqrt{\frac{1}{k}\sum_{i=1}^{n}z_i^2}\right)-\exp\left(\frac{1}{k}\sum_{i=1}^{n}\cos(2\Pi z_i)\right)+20+e$	*30,[–32, 32]*
Griewank	$f_{11}(z)=\frac{1}{4000}\sum_{i=1}^{k}z_i^2-\Pi_{i=1}^{n}\cos\left(\frac{zl}{\sqrt{i}}\right)+1$	*30,[–600, 600*
Penalized	$f_{12}(z)=\frac{\Pi}{k}\left\{101\sin(\Pi d_1)+\sum_{i=1}^{k-1}(d_i-1)^2[1+10\sin^2(\Pi d_{i+1})+(d_n-1)^2\right\}$ $+\sum_{i=1}^{n}v(z_i,10,100,4)$	*30,[–50, 50]*
	$where\ d_i=1+\frac{z_i+1}{4}\ \ and\ \ u(z_i,a,j,n)=\begin{cases}j(z_i-a)^n\ z_i\rangle a\\0-a\langle z_i\langle a\\j(-z_i-a)^m\ z_i\langle -a\end{cases}$	
Penalized 2	$f_{13}(z)=0.1\left\{\sin^2(3\Pi z_i)+\sum_{i=1}^{k}(z_i-1)^2[1+\sin^2(3\Pi z_i+1)]\right\}$ $+(z_i-1)^2[1+\sin^2(3\Pi z_k]$ $+\sum_{i=1}^{k}v(z_i,5,100,4)$	*30,[–50, 50]*
Foxholes	$f_{14}=\left(\frac{1}{500}+\sum_{i=1}^{25}\frac{1}{i+\sum_{j=1}^{2}(z_i-a_{ij})^6}\right)^{-1}$	*2, [-65.536,65.536]*
Kowalik	$f_{15}=\sum_{i=1}^{11}\left(a_i-\frac{z_1(b_i^2+b_iz_2)}{b_i^2+b_iz_3+z_4}\right)^2$	*4, [− 5,5]*
Six-hump *Camel-back*	$f_{16}(z)=4z_1^2-2.1z_1^4+\frac{1}{3}z_1^6+z_1z_2+4z_2^4$	*2, [− 5,5]*
Branin	$f_{17}(z)=\left(z_2-\frac{5}{4\pi^2}z_1^2+\frac{5}{\pi}z_1-6\right)^2+10\left(1-\frac{1}{8\pi}\right)\cos z_1+10$	*2, [− 5,5]*
Goldstein-Price	$f_{18}(z)=\left[1+(z_1+z_2+1)^2(19-14z_1+3z_1^2-14z_2+6z_1z_2+3z_2^2)\right]\times$ $30+(2z_1-3z_2)^2\times(18-32z_1+12z_1^2+48z_2-36z_1z_2+27z_2^2)$	*2, [− 5,5]*
Hartmen 3	$f_{19}(z)=-\sum_{i=1}^{4}c_i\exp\left(\sum_{j=1}^{3}a_{ij}(z_j-p_{ij})^2\right)$	*3, [− 5,5]*
Hartmen 6	$f_{20}(z)=-\sum_{i=1}^{4}c_i\exp\left(-\sum_{j=1}^{6}a_{ij}(z_j-p_{ij})^2\right)$	*6, [−5,5]*
Shekel 5	$f_{21}(z)-\sum_{i=1}^{5}\left[(Z-a_i)(Z-a_i)^T+c_i\right]^{-1}$	*3, [− 5,5]*
Shekel 7	$f_{22}(z)-\sum_{i=1}^{7}\left[(Z-a_i)(Z-a_i)^T+c_i\right]^{-1}$	*3, [− 5,5]*
Shekel 10	$f_{23}(z)-\sum_{i=1}^{10}\left[(Z-a_i)(Z-a_i)^T+c_i\right]^{-1}$	*3, [− 5,5]*

TABLE 3. Performance comparison of IMRFO with MRFO, GWO,SCA,BFO for the unimodal and modal benchmark functions.

Functions		IMRFO	MRFO	SCA	GWO	BFO
F1	AVG	0.00E+00	4.13E-08	2.77E-27	23.1034	1.82E-43
	SD	0.00E+00	6.32E-08	8.68E-27	23.6297	1.9E-43
	Med	0.00E+00	2.06E-08	2.27E-29	14.0483	1.56E-43
	Worst	0.00E+00	1.32E-08	4.59E-26	62.8736	7.9E-43
F2	AVG	0.00E+00	3.9953	1.27E-19	2.443	7.61E-26
	SD	0.00E+00	3.1452	3.05E-20	3.2216	7.12E-26
	Med	0.00E+00	4.0496	7.67E-23	2.8465	6.19E-26
	Worst	0.00E+00	9.856	7.94E-20	10.0076	2.72E-25
F3	AVG	0.00E+00	0.000000805	4.58E-08	95.5016	0.186
	SD	0.00E+00	0.00000109	0.000000128	52.5843	0.133
	Med	0.00E+00	0.000000208	3.95E-12	99.6219	0.131
	Worst	0.00E+00	0.00000282	0.000000407	173.7757	0.131
F4	AVG	0.00E+00	0.0000788	2.54E-09	8.6909	0.000000211
	SD	0.00E+00	0.0001037	5.46E-09	5.1829	8.88E-08
	Med	0.00E+00	0.000053	4.81E-11	8.0967	0.00000019
	Worst	0.00E+00	0.0003682	0.000000168	14.8275	0.000000339
F5	AVG	5.26E-08	931.2192	7.118	5021.7729	3.2
	SD	1.01E-07	2396.3352	0.25018	9520.2362	2.2
	Med	4.57E-09	135.1696	7.2289	937.3661	2.78
	Worst	3.27E-07	7710.4457	7.3661	2842.7823	6.68
F6	AVG	0.00E+00	6.71E-10	0.31179	31.0031	0.00E+00
	SD	0.00E+00	5.85E-10	0.11916	41.1201	0.00E+00
	Med	0.00E+00	5.33E-10	0.29383	16.4782	0.00E+00
	Worst	0.00E+00	3.13E-09	0.48389	125.0165	0.00E+00
F7	AVG	0.0000157	2.6014	0.0007298	0.014187	0.0028
	SD	0.0000141	1.8186	0.0005702	0.012918	0.00103
	Med	0.000012	2.3699	0.0006444	0.011674	0.0026
	Worst	0.0000531	4.853	0.0020895	0.040038	0.00478
F8	AVG	-2665.515	-1746.786	-2313.3951	-3986.0388	-4170
	SD	223.8271	264.2662	248.3506	1688.1824	50
	Med	-2634.759	-1766.228	-2197.3255	-3817.0586	-4190
	Worst	-2400.079	-1338.729	-2136.702	-2363.8598	-4070
F9	AVG	0.00E+00	22.4274	1.5968	24.7889	0.00E+00
	SD	0.00E+00	10.555	5.0495	10.6151	0.00E+00
	Med	0.00E+00	21.6892	6.65E-10	31.4845	0.00E+00
	Worst	0.00E+00	37.8168	15.9679	48.0048	0.00E+00
F10	AVG	8..79E-17	3.7958	3.5E-15	6.2984	5.55E-16
	SD	0.00E+00	6.1069	4.15E-14	2.2409	0.00E+00
	Med	9..99E-16	0.81329	8.07E-15	6.5454	5.55E-15
	Worst	9.09E-16	20.0102	2E-13	8.2954	5.55E-15
F11	AVG	0.00E+00	1.9127	0.090781	1.254	0.00074
	SD	0.00E+00	1.4079	0.19771	0.68186	0.00234
	Med	0.00E+00	1.3825	0.00000098	1.1417	0.00E+00
	Worst	0.00E+00	4.4141	0.61623	2.6858	0.0074
F12	AVG	4.71E-32	0.10412	0.070837	5.7617	4.71E-32
	SD	2.26E-48	0.43889	0.020720	6.7270	2.26E-48
	Med	5.82E-33	0.0000829	0.086773	5.362	5.81E-33
	Worst	5.82E-32	2.148	0.006228	27.4203	5.81E-33
F13	AVG	1.35E-32	0.010807	0.22513	9.4578	1.35E-32
	SD	3.98E-49	0.026982	0.08226	7.2843	3.90E-49
	Med	2.46E-33	0.0072202	0.35616	8.8634	2.46E-33
	Worst	2.46E-33	0.061285	0.43123	20.7563	2.46E-33
F14	AVG	0.998	0.998	1.5935	1.295	0.998
	SD	0.00E+00	2.4E-16	0.95823	0.93927	0.00E+00
	Med	0.998	0.998	0.99809	0.998	0.998
	Worst	0.998	0.998	2.9821	3.9683	0.998

TABLE 3. *(Continued.)* **Performance comparison of IMRFO with MRFO, GWO,SCA,BFO for the unimodal and modal benchmark functions.**

F15	AVG	0.0003828	0.002854	0.0008991	0.0058969	0.000749
	SD	0.000238	0.005865	0.000331	0.0036945	0.000191
	Med	0.0003075	0.001023	0.0007456	0.0054318	0.000718
	Worst	0.0010602	0.019529	0.0014997	0.013469	0.00122
F16	AVG	-1.03161	−1.0316	−1.0316	−1.0316	−1.03
	SD	0.00E+00	2.86E-14	0.000016	1.48E-16	0.00E+00
	Med	−2.14272	−2.1427	−2.1427	−2.1427	−1.03
	Worst	−2.14272	−2.1427	−2.1427	−2.1427	−1.03
F17	AVG	0.40890	1.02	0.39898	0.39871	0.398
	SD	0.00E+00	0.78951	0.0011636	0.0014329	0.00E+00
	Med	0.40890	0.62742	0.40946	0.40930	0.409
	Worst	0.40890	2.4202	0.40126	0.40274	0.398
F18	AVG	2	2	2	2	2
	SD	0.00E+00	1.85E-13	0.0000396	5.34E-16	2.96E-16
	Med	2	2	2	2	2
	Worst	2	2	2.0001	2	2
F19	AVG	−4.9739	– 4.9653	−4.9651	−4.9739	−4.97
	SD	0.00E+00	0.0007109	0.0007109	9.74E-17	9.47E-17
	Med	−4.9719	−4.9656	−4.9656	−4.9739	−4.97
	Worst	−4.9719	−4.964	−4.964	−4.9739	−4.97
F20	AVG	−3.2863	−3.262	−2.8029	−3.2735	−3.32
	SD	0.057431	0.063271	0.38047	0.061513	4.68E-16
	Med	−3.322	−3.2624	−3.0014	−3.3196	−3.32
	Worst	−3.2031	−3.2007	−1.9211	−3.1995	−3.32
F21	AVG	−10.1532	−6.1389	−3.0066	−8.8957	−10.1
	SD	0.00E+00	3.5821	2.2011	2.7143	0.078
	Med	−10.1532	−5.1008	−3.1737	−10.1532	−10.2
	Worst	−10.1532	−2.6305	−0.4982	−2.6305	−9.91
F22	AVG	−10.4029	−6.0514	−4.1502	−9.6392	−10.4
	SD	2.29E-16	3.0285	2.2208	3.526	2.43E-16
	Med	−10.4029	−3.9474	−4.707	−10.4029	−10.4
	Worst	−10.4029	−2.7519	−0.90936	−2.7659	−10.4
F23	AVG	−10.5364	−6.5631	−4.4381	−8.1416	−8.45
	SD	1.78E-15	4.191	0.97997	3.8574	3.43
	Med	−10.5364	−6.7038	−4.6828	−10.5364	−10.5
	Worst	−10.5364	−2.4217	−2.8115	−2.4273	−1.86

$$[H]_{n\times n} = \begin{bmatrix} \frac{\partial P_1}{\partial \theta_1} & \frac{\partial P_1}{\partial \theta_2} & \cdots\cdots & \frac{\partial P_1}{\partial \theta_n} \\ \frac{\partial P_2}{\partial \theta_1} & \frac{\partial P_2}{\partial \theta_2} & & \frac{\partial P_2}{\partial \theta_n} \\ \vdots & & & \\ \vdots & & & \\ \frac{\partial P_n}{\partial \theta_1} & \frac{\partial P_n}{\partial \theta_2} & \cdots\cdots & \frac{\partial P_n}{\partial \theta_n} \end{bmatrix}_{n\times n} \tag{11}$$

$$\begin{aligned}[\Delta\theta] &= [H]^{-1}[\Delta P] \\ &= [M][\Delta P] \end{aligned} \tag{12}$$

where,

$$[M] = [H]^{-1} \tag{13}$$

The values of M in Equation (13) needs to be found out in order to get the values associated with $\partial\theta_i/\partial P_{G_g}$ and $\partial\theta_j/\partial P_{G_g}$ in the Equation (3). $[H]$ resembles a singular matrix of rank one deficiency and cannot be directly invertible. In this work, the slack bus has been designated as number 1, thus the elements corresponding to the first row and first column of $[H]$ are neglected to form the $[H_{-1}]$ matrix, which is inverted to get the $[M_{-1}]$ matrix, where $()_{-1}$ resembles the matrix with its first row and column deleted. Thus, considering this relation the following mathematical relation can be represented:

$$[\Delta\theta_{-1}] = [M_{-1}][\Delta P_{-1}] \tag{14}$$

Adding the element $\Delta\theta_1$ to Equation (14) yields the actual vector $[\Delta\theta]$, and can be represented as:

$$[\Delta\theta]_{n\times 1} = \begin{bmatrix} 0 & 0 \\ 0 & [M_{-1}] \end{bmatrix}_{n\times n} [\Delta P]_{n\times 1} + \Delta\theta_1 \begin{bmatrix} 1 \\ 1 \\ . \\ . \\ 1 \end{bmatrix}_{n\times 1} \tag{15}$$

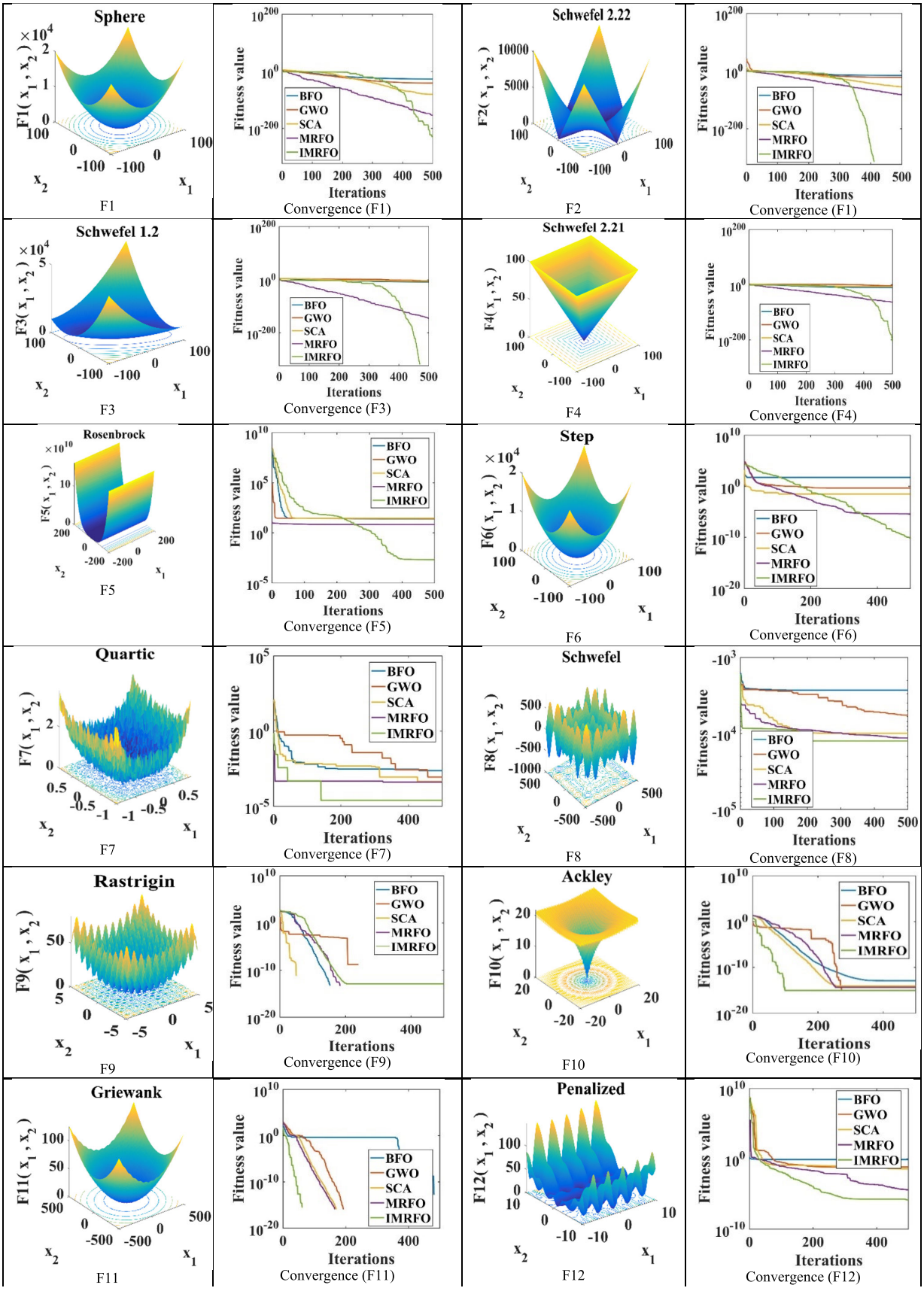

FIGURE 1. Comparative representation of unimodal and multimodal benchmark function and convergence profile for IMRFO with MRFO, GWO,SCA,BFO.

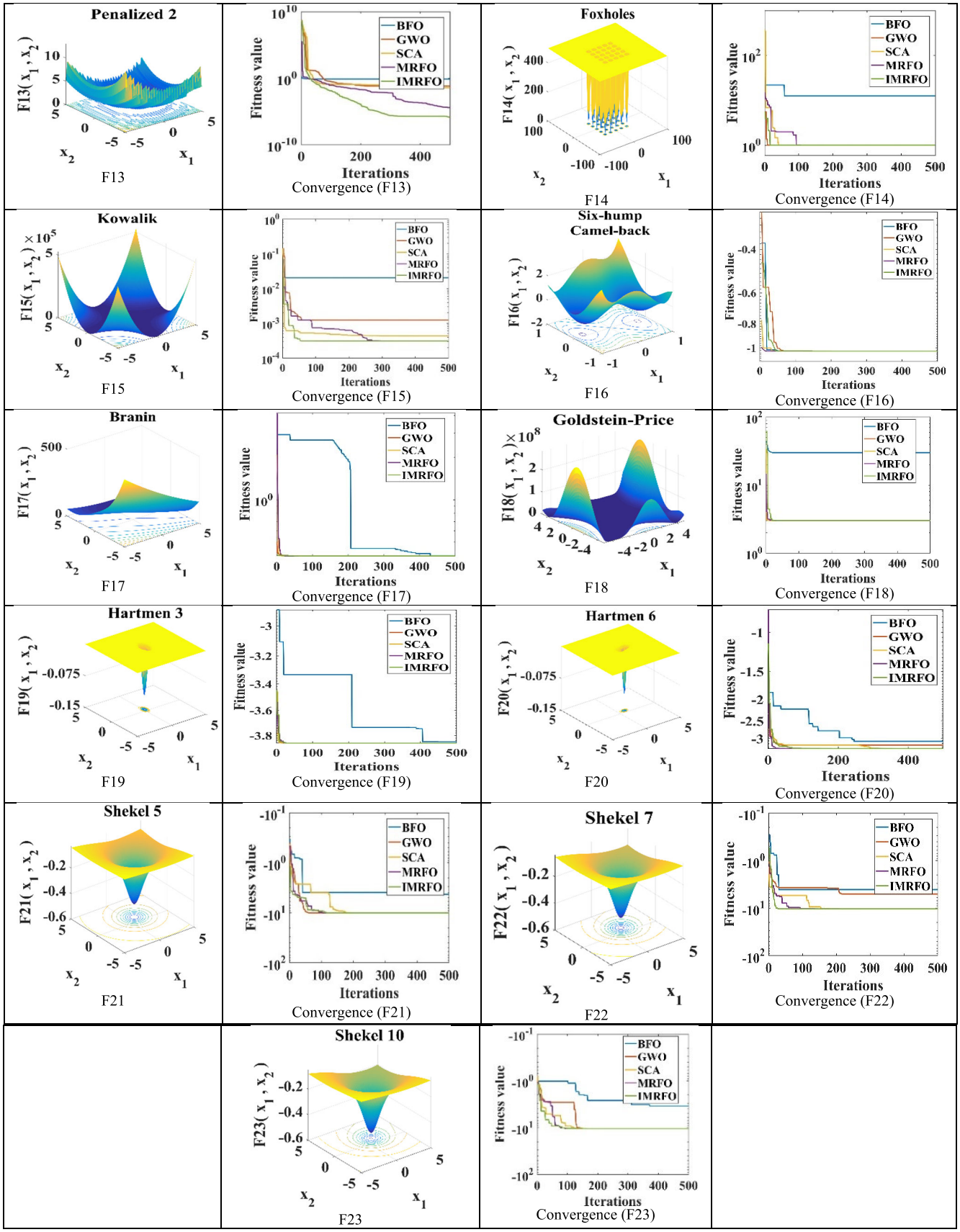

FIGURE 1. *(Continued.)* **Comparative representation of unimodal and multimodal benchmark function and convergence profile for IMRFO with MRFO, GWO,SCA,BFO.**

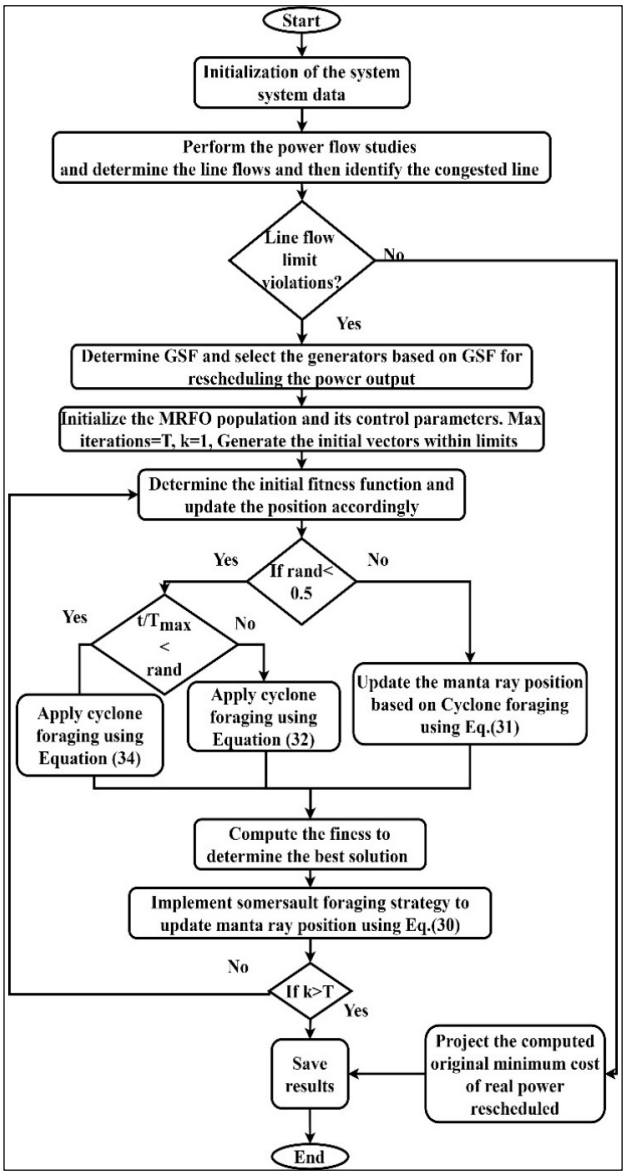

FIGURE 2. IMRFO flow chart for CM.

The second component of the mathematical expression in Equation (15) can be neglected as $\Delta\theta_1$, because the change in the phase angle corresponding to the slack is considered as zero. Thus, Equation (15) can be represented as:

$$[\Delta\theta]_{n\times 1} = \begin{bmatrix} 0 & 0 \\ 0 & [M_{-1}] \end{bmatrix}_{n\times n} [\Delta P]_{n\times 1} \tag{16}$$

The values corresponding to the elements $\partial\theta_i/\partial P_{G_g}$ and $\partial\theta_j/\partial P_{G_g}$ can be fetched from Equation (16). The GSF values is determined considering the slack bus as the reference bus. Thus, The GSF of the slack bus generator is zero for the congested line.

In the power system framework, the power delivery of all the generators does not create significant impact of the power flow of the congested lines. For a specific congested line, the power flow in it is highly influenced by the power delivery of some selective critical generators within the system. Thus, for effective performance only those selective generators are selected based on the GSF.

GSF represents the amount of active power flow that would vary along a congested transmission channel/path linking bus-i and bus-j as a result of small alteration in the real power injection by the g^{th} generator. ISO identifies the generators with the most deviated GSFs and engage those generators to participate in CM strategy by rescheduling their power outputs.

The minimization of the Congestion Cost (CC) is achieved by considering the price bids and optimal real power rescheduled by the generators participating in CM which can be

TABLE 4. Parameters for BFO, SCA, GWO, MRFO, IMRFO.

Optimization Techniques	Parameters
IMRFO	$r_i \in [0,1]$, $IF_1 = 2.5$, $IF_2 = 1.5$, S=2
MRFO [37]	$r_i \in [0,1]$,S=2
GWO [43]	$\alpha_{min} = 0$, $\alpha_{max} = 2$
SCA [44]	$\lambda_1 = 2.\ \lambda_2 = 2\pi * rand\ \ \lambda_3 = 2 * rand$ $\lambda_4 = rand$
BFO[45]	No. of Steps N_{step}=4, No. of chemo tactics steps N_{chemo_step}=100. Reproduction steps N_{re}=4, Probability =0.2

Algorithm 1 Pseudocode of IMRFO for CM

```
Initialize the manta ray population size NP=30.
Set the maximum iteration T=300
Compute the fitness for search agents and determine the best solution x_best
while (iterations< maximum iterations) do
    for i=1 to NP do
        if (rand<0.5) then // Cyclone foraging
            if (iter/iter_max < rand) then
            Update position of the search agent by Equation (33)
            else
            end if
        else // Chain foraging
        Position update using Equation (32)
        end if
    Determine the individual fitness values corresponding to each of the search agents
    then Update x_best in case there exists a better solution
    //Somersaulting foraging
    for i=1 to NP do
    Update the search agent position using Equation (29)
    Compute the fitness for each individual
    then Update x_best in case of better solution
    end for
    iteration=iteration+1
end while
Return the best solution
```

represented as:

$$CC = \text{minimize} \sum_{g=1}^{N_g} C_g(\Delta P_g)\Delta P_g \tag{17}$$

Here in Equation (17), C_g represents the generator's price bids in ($/MWh), ΔP_g resembles the adjustment in the amount of the real power at the bus g and N_g states the total number of participating generators in CM.

Constrains for the proposed CM optimization problem:

$$\sum_{g=1}^{N_g}((GSF_g) * \Delta P_g) + PF_k^0 \leq PF_k^{\max} \tag{18}$$

$$\Delta P_g^{\min} \leq \Delta P_g \leq \Delta P_g^{\max} \tag{19}$$

$$\Delta P_g^{\min} = P_g - P_g^{\min} \tag{20}$$

$$\Delta P_g^{\max} = P_g^{\max} - P_g \tag{21}$$

$$\sum_{g=1}^{N_g} \Delta P_g = 0 \tag{22}$$

Here $P_g^{\max}$ and $P_g^{\min}$ are the maximum and minimum power generating boundaries of the generators. PF_k^0 and $PF_k^{\max}$ are the actual power flow in the kth line and the maximum power flow of the kth line respectively. The solutions of the power flows are not necessarily required during the optimization process. In the CM optimization problem, Equation (22) handles the power balance scenario, except accounting for the losses. After the complete execution of the optimization process the allocation of real power generation is done at the slack bus which addresses the system losses. The details execution is represented as:

Step1: Run load flow and find out the congested lines.

Step 2: Fetch the values of the parameters from load flow solutions that are required for the optimization process (this also includes the incorporation of the upper limit and lower limit of the system constrains that are required for the optimization problem).

Step 3: Run the optimization process with the incorporation of the load flow parameters in it. Compute the objective function as the congestion cost in the optimization process while satisfying the Equality and In equality constrains.

Step 4: At the end of the optimization process, fetch the optimal system parameters from the optimization process and feed them independently to the load flow routine ones again to verify whether the parameters are satisfying the test system constraints.

III. MANTA RAY FORAGING OPTIMIZATION

The Manta Ray Foraging Optimization (MRFO) has been developed by Zhao et al. in the year 2020. The framework of the MRFO has been developed from the foraging behaviour of manta ray [37]. The MRFO framework is based on the three-foraging behaviour (chain, cyclone, and somersault) of manta ray. Like the other swarm inspired optimization approaches, MRFO also generates its population in a randomly within the vicinity of the search space. The updating mechanism for these generated population is performed based on the three-foraging methodology (chain, cyclone and somersault foraging).

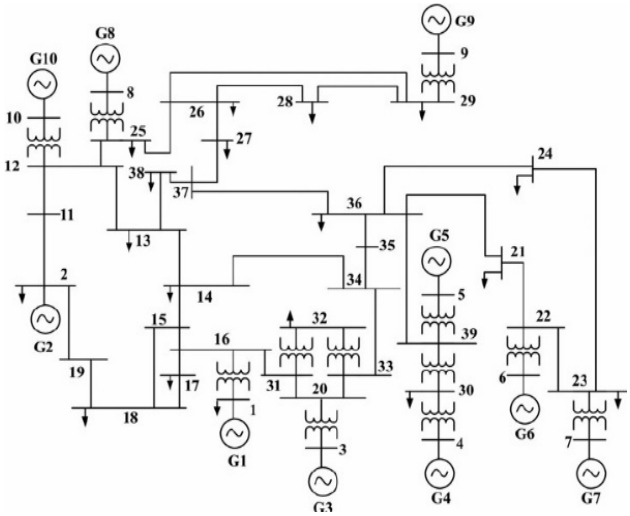

FIGURE 3. Test system framework of 39-bus new england system.

TABLE 5. Generator sensitivity factors for the congested line L(15-16).

Gen No.	1	2	3	4	5
GSF	0.00	-0.58	-0.06	-0.26	-0.26
Gen No.	6	7	8	9	10
GSF	-0.26	-0.26	-0.61	-0.55	-0.61

A. CHAIN FORAGING

The manta rays link their head and tail to a systematic line to develop the foraging chain. The best solution for the MRFO is projected based on the higher concentration of plankton which signifies the target prey. Maintaining the foraging chain, the group of manta ray individuals follow the first manta ray individual, that moves forward and traces the path for the food. The chain foraging can be stated as:

$$x_i^{t+1} = \begin{cases} x_i^t + r_1(x_{best}^t - x_i^t) + \\ \alpha(x_{best}^t - x_i^t), & i = 1 \\ x_i^t + r_2(x_{i-1}^t - x_i^t) + \\ \alpha(x_{best}^t - x_i^t), & i = 2, 3, \ldots .NP \end{cases} \tag{23}$$

$$\alpha = 2 \cdot r_3 \cdot \sqrt{|\log(r_4)|} \tag{24}$$

Here in Equation (23) x_i^t denotes the i^{th} individual position at t^{th} generation. r_i is the random vector ranging from [0,1] for the i = 1,2,3,4. x_{best} resembles the best optimal individual which signifies the highest concentration of plankton. The population number is denoted as NP and α as the weighted coefficient.

B. CYCLONE FORAGING

The manta rays whenever locate the plankton underneath the ocean water, they travers towards the food in the form of

TABLE 6. Representation of results opted with Gradient method, IMRFO, MRFO, SCA, GWO, and BFO for 39-bus system.

	RED [16]	PSO [19]	ABC [26]	Gradient method [solved]	BFO [solved]	GWO [solved]	SCA [solved]	MRFO [solved]	IMRFO [proposed]
Approx. Congestion Cost of rescheduling ($/h)	8639.17	8872.9	8456	8904.26	8363.46	8135.36	7956.14	7348.16	7018.28
Best Approx. congestion Cost ($/h)	NR	NR	NR	8904.26	8363.46	8135.36	7956.14	7348.16	7018.28
Worst Approx. congestion cost ($/h)	NR	NR	NR	NR	12180.43	9692.07	8841.31	7801.52	7205.08
Mean value	NR	NR	NR	NR	10472.81	8677.50	8309.31	7518.49	7152.63
Line 15-16 power flow (MW) (after CM)	510	490.00	499.50	499.46	496.90	499.10	496.98	496.90	499.00
ΔP_1 (MW)	-99.59	-149.1	-131.0	-151.84	-131.36	-129..28	-159.97	-141.98	-143.27
ΔP_2(MW)	98.75	65.6	63.2	36.28	45.21	44.34	66.03	59.27	34.85
ΔP_3(MW)	-159.64	-129	-132.0	-136.17	-124.23	-123.96	-89.02	-99.60	-120.46
ΔP_4(MW)	12.34	NI	NI	NI	NI	NI	NI	NI	NI
ΔP_5(MW)	24.69	NI	NI	NI	NI	NI	NI	NI	NI
ΔP_6(MW)	24.69	NI	NI	NI	NI	NI	NI	NI	NI
ΔP_7(MW)	12.34	NI	NI	NI	NI	NI	NI	NI	NI
ΔP_8(MW)	24.69	75.4	72.2	94.4	89.87	87.09	62.34	69.57	61.02
ΔP_9(MW)	12.34	52.1	49.1	51.42	46.59	46.59	52.93	39..86	42.02
ΔP_{10}(MW)	49.38	83	78.8	80.18	77.91	71.62	70.60	69.87	71.62
Total Amount (MW)	518.45	554.2	526.3	550.29	515.17	502.88	500.89	480.15	473.24
Note: NR=Not reported, NI=Not involve									

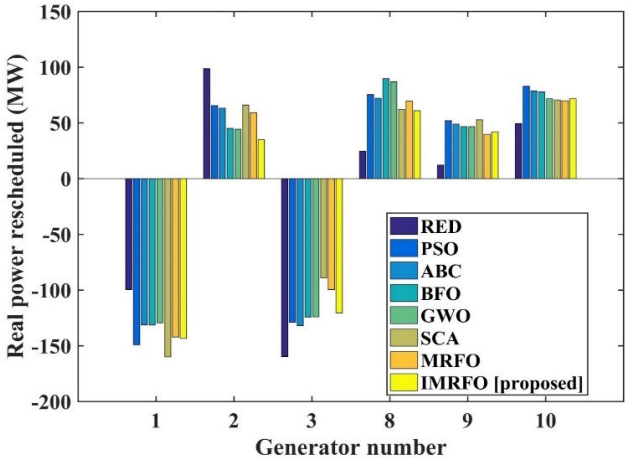

FIGURE 4. Rescheduled real power with RED [16], PSO [19], ABC [26], SCA [solved], GWO [solved], BFO [solved], MRFO [solved], and IMRFO for 39-bus system.

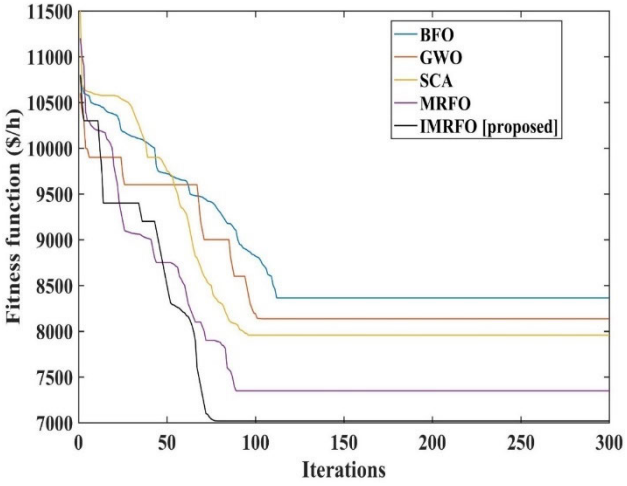

FIGURE 5. Convergence profile for BFO, GWO, SCA, MFRO, and IMRFO for CM.

a spiral while maintaining the long chain while tracing the movement of the front individual (manta ray). The mathematically representation of the cyclone foraging is as follows:

$$x_i^{t+1} = \begin{cases} x_{best}^t + r_5(x_{best}^t - x_i^t) + \\ \beta(x_{best}^t - x_i^t), & i = 1 \\ x_{best}^t + r_6(x_{i-1}^t - x_i^t) + \\ \beta(x_{best}^t - x_i^t), & i = 2, 3, \ldots .NP \end{cases} \tag{25}$$

$$\beta = 2 \cdot \exp(r_7 \cdot (iter_{\max} - iter + 1)/iter_{\max}) \cdot \sin(2\pi r_7) \tag{26}$$

Here in Equation (25), r_i is the uniformly distributed random vector in the range [0,1] and i =5,6. β signifies the weighted coefficient. In Equation (26) r_7 is a random number in the range [0,1]. *iter* is the current iteration count and $iter_{\max}$ is the maximum iterations.

Equation (25) signifies that the food is primarily employed as a locus for spiral foraging. This allows the exploitation of the search space within the close location of the food. Thus, to extend the searching capacity, a randomly generated location is selected within the region of the search area which acts as the locus of the spiral foraging. This allow the manta

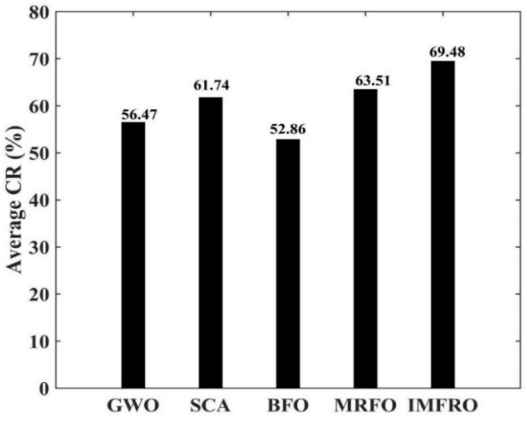

FIGURE 6. Representation of CR values for SCA [solved], GWO [solved], BFO [solved], MRFO [solved], and IMRFO for CM (39-bus system).

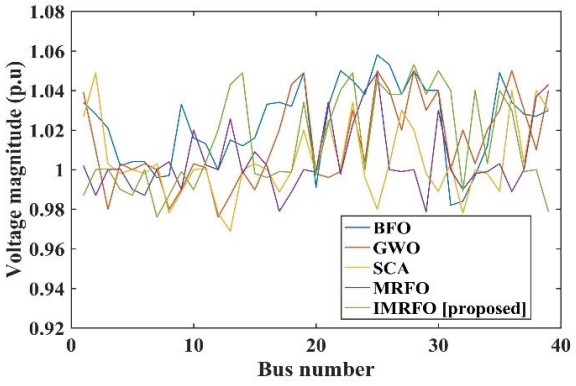

FIGURE 7. Representation of comparative system voltage profile for 39 bus system with BFO, GWO, SCA, MFRO, and IMRFO.

rays to look for better regions that are far away from their present best position.

In the manta ray framework of optimization, the mechanism of random spiral foraging is primarily concerned with exploration, thus, promoting a tendency of global search for MRFO. The mathematical model is represented as:

$$x_{rand} = lb + r_8 \cdot (ub - lb) \tag{27}$$

$$x_i^{t+1} = \begin{cases} x_{rand} + r_9(x_{best}^t - x_i^t) + \\ \beta(x_{best}^t - x_i^t), & i = 1 \\ x_{rand} + r_{10}(x_{i-1}^t - x_i^t) + \\ \beta(x_{best}^t - x_i^t), & i = 2, 3, \ldots .NP \end{cases} \tag{28}$$

Here in Equation (27) x_{rand} is a random position and $r_i \in [0, 1]$. The upper boundary and the lower boundary of the area of the search space is designated as *ub* and *lb* respectively.

C. SOMERSAULTING FORAGING

In this stage, the location of the food is regarded as the pivot point. Each of the manta ray rotates around the pivot searching for a new spot. This phase is mathematically represented as:

$$x_i^{t+1} = x_i^t + S \cdot (r_{11} \cdot x_{best}^t - r_{12} \cdot x_i^t), \quad i = 1, 2, \ldots .NP \tag{29}$$

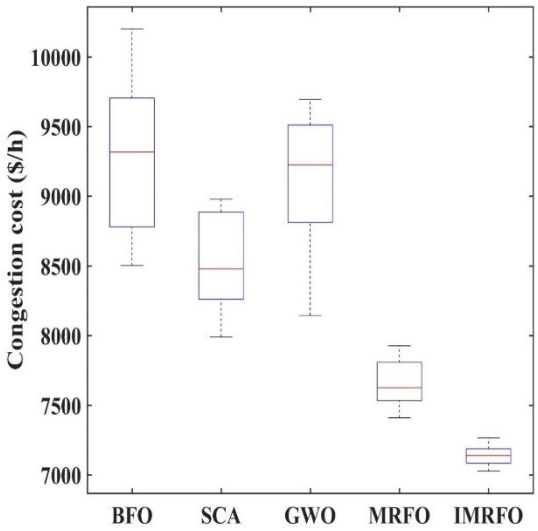

FIGURE 8. Box plot for BFO, GWO, SCA, MFRO, and IMRFO for the congestion costs for 39-bus system.

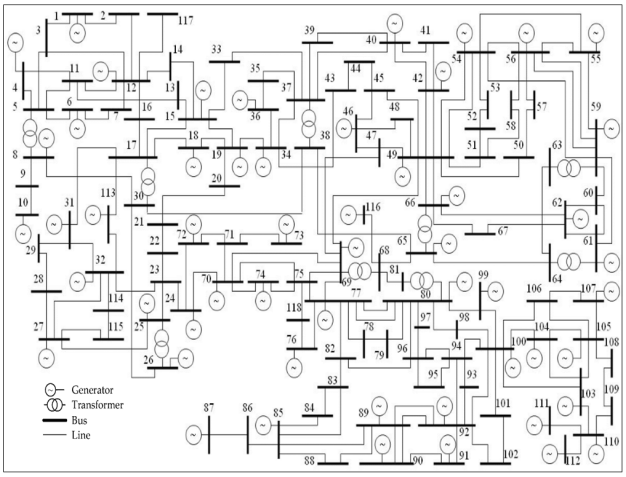

FIGURE 9. Representation of IEEE-118 bus system.

TABLE 7. Computational time for RED [16], PSO [19], ABC [26], SCA, GWO, BFO, MRFO, and IMRFO.

	Average Computational Time (Sec)				
	BFO [solved]	GWO [solved]	SCA [solved]	MRFO [solved]	IMRFO [proposed]
Iterations /Trials	300/30	300/30	300/30	300/30	300/30
Time (Sec.)	8.53	8.65	7.49	7.37	6.46

Here in Equation (29), S is designated as the somersault factor that determine the somersault range for the manta rays; based on test run the value of S is taken as 2. r_{11} and r_{rr} lies in the range [0,1].

The MRFO governs the phases of exploitation and exploration behaviours by modulating the transformation of $iter/iter_{\max}$. During the scenario when $(iter/iter_{\max}) < rand$, the execution of exploration behaviour is conducted, and the sources of the food are generated in the random manner in the location the search region. During the optimization

TABLE 8. System parameters representation post CM with RED [16], PSO [19], ABC [26], SCA, GWO, BFO, MRFO, and IMRFO.

Parameters	RED [16]	PSO [19]	ABC [26]	BFO [solved]	GWO [solved]	SCA [solved]	MRFO [solved]	IMRFO [proposed]
P_{Loss} (MW)	58.00	57.60	58.73	58.81	58.09	58.35	57.87	57.31
V (p.u)	0.9324	0.9407	0.9480	0.9680	0.9640	0.9637	0.9760	0.9896

TABLE 9. GSF values (118-bus system).

Gen No.	1	4	6	8	10	12	15	18	19
GSF	0	0.002	-0.002	-0.03	-0.03	-0.03	-0.03	-0.03	-0.03
Gen No.	24	25	26	27	31	32	34	36	40
GSF	-0.03	-0.03	-0.04	-0.39	-0.19	0.47	0.56	0.53	0.49
Gen No.	42	46	49	54	55	56	59	61	62
GSF	0.02	0.02	0.03	0.007	0.006	0.005	0.006	-0.002	-0.006
Gen No.	65	66	69	70	72	73	74	76	77
GSF	-0.006	-0.005	-0.005	-0.07	-0.006	-0.015	-0.015	-0.004	-0.007
Gen No.	80	85	87	89	90	91	92	99	100
GSF	-0.005	-0.005	-0.006	-0.005	-0.0003	-0.0004	-0.0002	-0.0002	-0.0001
Gen No.	103	104	105	107	110	111	112	113	116
GSF	0.003	-0.001	-0.001	-0.002	-0.002	-0.004	-0.004	-0.003	-0.002

TABLE 10. Representation of results opted with IMRFO, MRFO, SCA, GWO, Gradient method, and BFO (118-bus test system).

	PSO [19]	Gradient method [solved]	BFO [solved]	GWO [solved]	SCA [solved]	MRFO [solved]	IMRFO [proposed]
Approx. Congestion Cost of rescheduling ($/h)	3890.57	4156.74	3778.63	3426.58	3218.44	3102.82	2890.16
Best Cost ($/h)	NR	NR	3778.63	3426.58	3218.44	3102.02	2890.16
Worst cost ($/h)	NR	NR	5814.02	4491.56	4163.12	3868.74	3217.03
Mean value	NR	NR	4164.81	36601.7	3361.98	3310.21	3118.57
Line 8-30 (MW) power flow post CM	199.56	199.03	199.00	198.98	198.90	198.90	198.09
ΔP_{69} (MW)	-3.79	-5.80	-2.99	-3.17	-3.06	-2.18	-2.07
ΔP_{27}(MW)	81.9	96.15	81.51	76.52	72.53	77.01	70.64
ΔP_{31}(MW)	16.4	12.90	15.94	18.62	15.07	13.02	11.17
ΔP_{32}(MW)	-17	-21.76	-17.54	-12.36	16.69	-16.56	-12.02
ΔP_{34}(MW)	-55	-46.04	-48.84	-42.02	-46.68	-38.09	-32.24
ΔP_{36}(MW)	-9	-16.38	-12.80	-12.17	10.04	-13.06	-11.68
ΔP_{40}(MW)	-16.3	-21.54	-14.60	-15.87	14.20	-.12.37	-10.39
Total Amount (MW)	199.39	220.57	194.22	180.73	178.27	172.29	150.21

process, when $(iter/iter_{\max}) > rand$, the optimal candidate solution is considered as the reference point, that aids in the accomplishment of the exploitation phenomenon. In association to this a random variable is considered to implement the process of spiral/chain foraging and sequentially the somersault foraging is executed in the complete process.

IV. IMPROVED MANTA RAY FORAGING OPTIMIZATION (IMRFO)

The MRFO suffers from the insufficient ability of exploitation, diminishing population diversity, and easily getting trapped into local optima. These shortcomings are basically generated due to the improper balance between the exploration and exploitation phases. Thus, to overcome these deficiencies, the mutual coordination between the phases of exploration and exploitation in IMRFO has been enhanced with the incorporation of improvement factors.

In the conventional MRFO, during its initial phase of execution, the group of plankton is considered as the best solution. This acts as the target for the other manta rays. In this scenario, the search agents update their position as the latest best position using the Equation (23). In the initial phase of MRFO as the best location of the search agent is not known, the formerly stated updating mechanism may lead to the convergence towards the position of the local optima. In MRFO during the search mechanism, the change in the position vector is governed by large steps which may lead to the inefficient exploration of the search space. Thus, in the conventional MRFO search mechanism, two improvement factors; IF_1 and IF_2 are introduced to enhance its

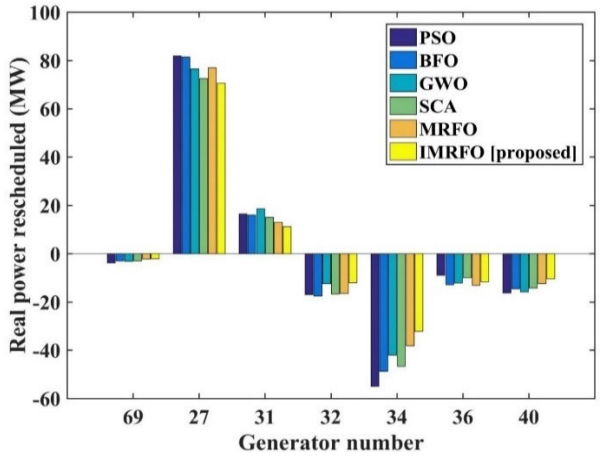

FIGURE 10. Power rescheduled with BFO, GWO, SCA, MRFO, IMRFO (118 bus test system).

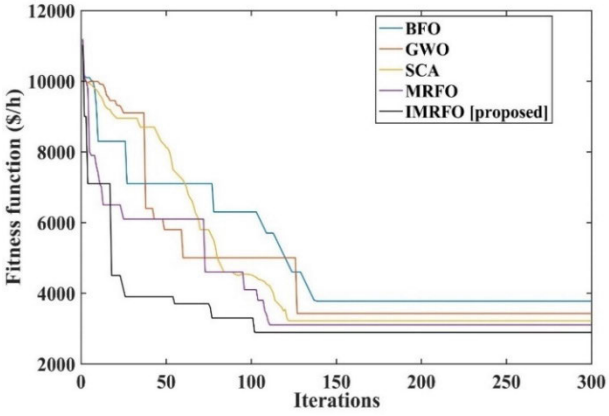

FIGURE 11. Convergence characteristics for BFO, GWO, SCA, MRFO, and IMRFO (118 bus test system).

performance. The modified mathematical representation for the IMRFO can be represented as:

$$G = \left|\alpha(x_{best}^{t} - x_i^t)\right| / IF_1 \tag{30}$$

$$x_{i(\bmod ified)}^{t+1} = \begin{cases} (x_i^t + r_1(x_{best}^t - x_i^t) + \\ \alpha(x_{best}^t - x_i^t))/IF_1, & i = 1 \\ (x_i^t + r_2(x_{i-1}^t - x_i^t) + \\ \alpha(x_{best}^t - x_i^t))/IF_1, & i = 2, 3, \ldots .NP \end{cases} \tag{31}$$

The inclusion of the improvement factors aids the manta ray to traverse in small steps towards the plankton concentration while effectively searching the search space. In Equation (23), the expression $\alpha(x_{best}^t - x_i^t)$ signifies the distance measured between the manta rays and the best solution in which has been modified to Equation (30) and the improved chain foraging mechanism is represented in Equation (31).

The exploitation phase is enhanced with the incorporation of improvement factors and the modified spiral updating

TABLE 11. Representation of system parameters with IMRFO, BFO, GWO, SCA, and MRFO for 118 bus system.

Parameters	BFO [solved]	GWO [solved]	SCA [solved]	MRFO [solved]	IMRFO [proposed]
P_{Loss} (MW)	138.93	138.77	137.56	137.81	136.63
V_{min} (p.u)	0.9649	0.9651	0.9634	0.9760	0.9786

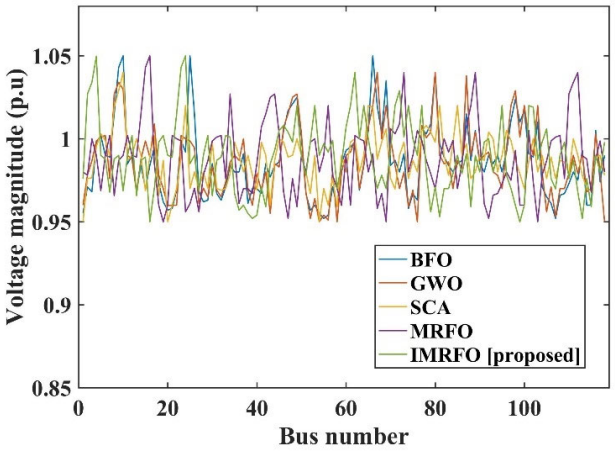

FIGURE 12. Comparative representation of voltage profile with BFO, GWO, SCA, MRFO, and IMRFO (118 bus test system).

TABLE 12. Computational time representation for IMRFO BFO, GWO, SCA, and MRFO (118 bus test system).

	Computational Time(Sec)				
	BFO [solved]	GWO [solved]	SCA [solved]	MRFO [solved]	IMRFO [proposed]
Iterations /Trials	300/30	300/30	300/30	300/30	300/30
Time (Sec.)	18.35	18.01	17.09	16.63	15.92

mechanism is represented as:

$$x_{i(\bmod ified)}^{t+1} = \begin{cases} (x_{best}^t + r_5(x_{best}^t - x_i^t) + \\ \beta(x_{best}^t - x_i^t))/IF_2, & i = 1 \\ (x_{best}^t + r_6(x_{i-1}^t - x_i^t) + \\ \beta(x_{best}^t - x_i^t))/IF_2, & i = 2, 3, \ldots .NP \end{cases} \tag{32}$$

In Equation (32), the improvement factors enhances the phase of exploitation by shrinking the spiral within which the manta ray searches the plankton, thus improving the exploitation behavior of the optimization algorithm.

In case of the conventional MRFO, during the exploration stage, the search agent position update is performed based on the Equation (28). This may result in the random movement of the manta ray. Thus, this scenario in conventional MRFO is take care for the search agent position update with the incorporation of the improvement factors in the exploration stage and the modified Equation (33) is represented as:

$$H = \left|\beta(x_{rand}^t - x_i^t)\right| / IF_1 \tag{33}$$

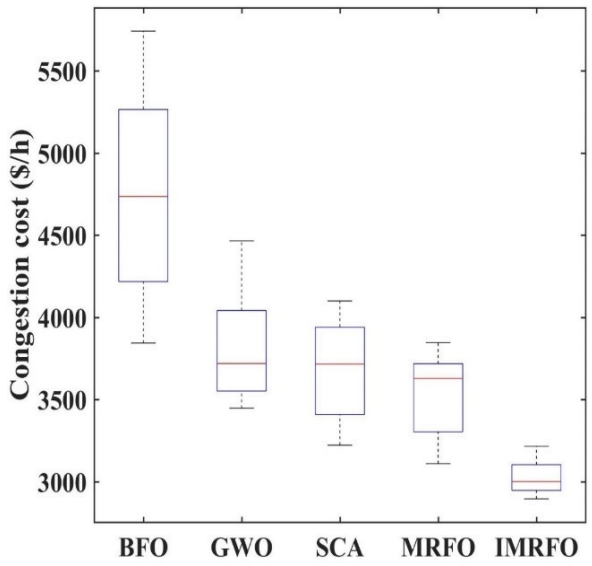

FIGURE 13. Box plot for BFO, GWO, SCA, MFRO, and IMRFO for the generated congestion costs for 118-bus system.

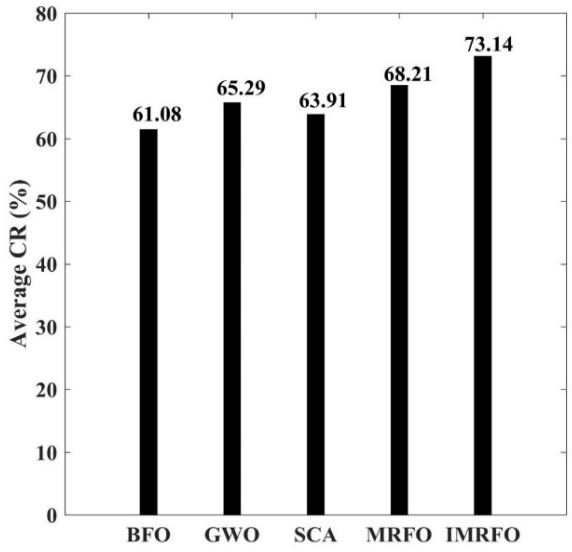

FIGURE 14. Representation of CR values for BFO, GWO, SCA, MFRO, and IMRFO (118-bus system).

$$x_{i(\text{mod}ified)}^{t+1} = \begin{cases} (x_{rand} + r_9(x_{best}^t - x_i^t) + \\ \beta(x_{best}^t - x_i^t))/IF_2, & i = 1 \\ x_{rand} + r_{10}(x_{i-1}^t - x_i^t) + \\ \beta(x_{best}^t - x_i^t)/IF_2, & i = 2, 3, \ldots .NP \end{cases} \tag{34}$$

The improvement factors IF_1 and IF_2 are taken as 2.5 and 1.5, respectively, which has been considered based on several number of trail runs.

A. PERFORMANCE EVAUATION OF IMRFO

The performance of the IMRFO has been measured on the 23 standard benchmark functions that constitutes of the seven unimodal and thirteen multimodal functions. The benchmark function ranges, formulas, optimal solutions, and dimension are all specified in [32]. The benchmark functions' details are listed in Table 1 and Table 2. Outputs achieved with IMRFO are contrasted to those outcomes obtained using other well-known metaheuristic methods such as BFO, SCA, GWO and the original MRFO. In the research, the search agents and the maximum iteration are set to 30 and 500, respectively, and the findings are acquired for 30 separate runs. The comparative results highlight that IMRFO has shown appreciable performance in the exploration and exploitation stages. The average (Avg) and standard deviation (SD), Med (median) and Worst (worst of the best-so-far solution) values obtained for IMRFO, BFO, SCA, GWO and the original MRFO in the last repetition has been stated in Table 3. The convergence profile of the 23 benchmark functions with IMRFO, MRFO, SCA, GWO, BFO has been represented in Figure 1. The pseudocode for IMRFO for CM is represented in Algorithm 1. IMRFO flow chart for the proposed CM problem has been portrayed in Figure 2.

V. RESULT ANALYSIS AND DISCUSSION

The IMRFO has been implemented for the proposed CM strategy using MATLAB 2016(a) software on a personal computer configuration of 8GB RAM, 3.10 GHz processor and Windows 11 operating system. The computational outcomes and the achieved results are analysed and compared under the same technical environment. The effectiveness of the CM has been examined using 39 bus New England, and a larger power system network of IEEE-118 bus system. Comparative analysis of results archived with IMRFO for the CM optimization problem has been illustrated with the existing referred algorithms, RED [16], PSO [19], ABC [26]. The contingencies like multiline contingencies, generator outage, wheeling transactions can also be considered in this research work but in order to establish an effective comparison on similar technical ground with research article RED [16], PSO [19], ABC [26] the line outage contingencies that are adopted in these article RED [16], PSO [19], ABC [26] have been considered in this proposed research. The proposed approach has also been solved with recent optimization algorithms like Gradient method [solved], BFO [solved], GWO [solved], SCA [solved], and original MRFO [solved] and compared with that of the results achieved with IMRFO to portray the effectiveness of IMRFO for the CM problem. The parameters of IMRFO, MRFO, GWO,SCA, and BFO are given in Table 4. The price bids of the generators for 39 bus system and 118 bus system have been represented in Table 13, and Table 14 in the Appendix section. The authors/researchers in RED [16], PSO [19], ABC [26] have considered different generators price bids in their work for the computation of congestion cost. So, to establish an uniform comparative platform the generator price bids stated in Table 13, and Table 14 have been considered for all the comparative cases to compute the results for comparison. The population size corresponding to the IMRFO and the other implemented optimization techniques has been taken as 30.

TABLE 13. Price bids for 39 bus new england system [47].

Gen No	1	2	3	4	5
Bids ($/Mwh)	11	17	19	20	15
Gen No	6	7	8	9	10
Bids ($/Mwh)	10	16	18	17	20

The complete execution of the optimization process has been executed for30 independent trials with 300 iterations.

A. 39-BUS NEW ENGLAND SYSTEM

The outline of this test system has 10 buses as the generator buses with 29 load buses. Figure 3 represents the single line diagram for the 39-bus New England System [46]. The line L(14-34) joining the buses 14-34 has been tripped. This tripping of the line L(14-34) has resulted congestion in the line L(15-16) with the increase in power flow to 628.2 MW (Line limit 500MW).

The GSFs are considered for the selection of the most responsive generators that would vary their power output to modulate the congested line power flow. The generators showing the most deviated or the most non-uniform GSFs are considered for power rescheduling as they would significantly impact the power flowing in the congested line. The GSFs computed are highlighted in Table 5. GSF values of the generators G4,G5, G6, and G7 are uniform and will not involve in the CM strategy, whereas the generators G2,G3,G8,G9, and G10 exhibits non-uniform GSFs and are considered for managing the congestion.

Table 6 highlights the results obtained with the application of the proposed IMRFO approach to solve the CM issue. Table 6 also includes the results obtained using RED [16], PSO [19], ABC [26], Gradient method [solved], SCA [solved], GWO [solved], BFO [solved], and original MRFO [solved] to represent a comparative effectiveness of the output achieved with IMRFO. Congestion cost of 7018.28$/h has been attained with application of the IMRFO, which is observed to be most economical in comparison to the other adopted techniques that are portrayed in Table 6. The real power rescheduled for the CM are also represented in Table 6. The total amount of the real power rescheduled with IMRFO is minimum among RED [16], PSO [19], ABC [26], Gradient method [solved], SCA [solved], GWO [solved], BFO [solved], and original MRFO [solved] that are applied for CM. The comparative representation of the real power rescheduled is highlighted in Figure 4.

The convergence characteristics achieved with IMRFO, and other optimization techniques has been represented in Figure 5. IMRFO has converged at 78^{th} iteration as compared to the other implemented techniques to deliver the optimal solution. The comparative convergence mobility analysis based on the Convergence Rate (CR) has been portrayed in Figure 6. IMRFO has the highest convergence rate among SCA [solved], GWO [solved], BFO [solved], and original MRFO [solved] for the CM. The comparative computational time of SCA, GWO, BFO, MRFO, and IMRFO are represented in Table 7 and 1 MRFO has appreciably lower computational time. Table 8 highlights the comparative system loss achieved with the optimization techniques after CM. The system loss achieved with IMRFO after CM is 57.31 MW which is appreciably lower than the system loss of 59.98 MW at the time of congestion. The system loss attained with IMRFO is also minimum among all the optimization techniques considered for alleviating congestion. Table 8 also shows the per unit (p.u) system voltages scenario after the CM. The system voltage achieved with IMRFO after CM is 0.9896 p.u and is appreciable in contrast to the other techniques applied for CM. The comparative system voltages profiles with the applied optimization approaches has been represented in Figure 7. Figure 8 characterises the box plot generated for the achieved congestion costs with SCA, GWO, BFO, MRFO, and IMRFO for 30 trials. The performance of IMRFO is comparatively appreciable than SCA, GWO, BFO, and MRFO.

B. 118-BUS SYSTEM

The IEEE 118-bus system has been considered to analyze the CM approach on a large power network. There are a total of 54 buses that are the generator buses and 64 buses that are marked as the load buses. Figure 3 represents the single line diagram of the 118-bus system. The line L(8-5) in 118 bus system has been tripped to create a congestion in the line L(8-30).

The GSFs determined for the overburdened line L(8–30) are provided in Table 9. The GSFs for generators G27, G31, G32, G34, G36, and G40 bears the most deviated GSF values. The generator G31 has the most negative GSF value and G34 has the highest positive GSF. As a result, generators G27, G31, G32, G34, G36, and G40 have been chosen to participate in CM. The slack bus generator has been selected to take part in the rescheduling procedure in order to diminish system losses. Thus, with the GSF approach, the participation of the generators for CM has been abridged to 7 generators from 54 generators. It is noticeable that with the GSF approach, the number of generators whose power outputs must be rescheduled to control congestion has decreased dramatically. The participating generators may be categorized into two sections considering the GSF values; positive GSF implies that increasing the generator's power output raises the power flow in the congested line, whereas a negative GSF shows that increasing the generators power output lowers the congested line power flow.

IMRFO has been applied to adjust the real power delivery by the generators in order to completely relieve the 62 MW overload from the congested line. Table 10 lists the output achieved with the implantation of the CM approach. The cost of rescheduling achieved to alleviate congestion using the IMRFO strategy has been 2890.16 $/h, which is appreciably economical than the other alternatives implemented for the CM. The congested line power flow with IMRFO has been curtailed to 198.09 MW and is below its maximum

TABLE 14. Price bids for 118 bus system [48].

Gen No.	1	4	6	8	10	12	15	18	19
Bids ($/Mwh)	11	25	19	16	21	12	13	14	17
Gen No.	**24**	**25**	**26**	**27**	**31**	**32**	**34**	**36**	**40**
Bids ($/Mwh)	19	70	15	17	19	20	15	10	18
Gen No.	**42**	**46**	**49**	**54**	**55**	**56**	**59**	**61**	**62**
Bids ($/Mwh)	14	10	20	21	13	18	16	15	17
Gen No.	**65**	**66**	**69**	**70**	**72**	**73**	**74**	**76**	**77**
Bids ($/Mwh)	19	25	60	15	14	17	9	6	20
Gen No.	**80**	**85**	**87**	**89**	**90**	**91**	**92**	**99**	**100**
Bids ($/Mwh)	18	17	19	22	18	19	10	21	30
Gen No.	**103**	**104**	**105**	**107**	**110**	**111**	**112**	**113**	**116**
Bids ($/Mwh)	15	14	11	20	21	22	23	19	25

power flow limit. Table 10 shows that the overall amount of active power rescheduling accomplished using IMRFO is 150.21 MW, and appreciably lower as compared to that with than with PSO, BFO, GWO, SCA, and MRFO. Table 10 shows the real power rescheduled using IMRFO and other approaches.

Figure 11 depicts the convergence profile for the implanted optimization techniques for CM. The IMRFO converged at 112^{th} iteration as compared to the other considered CM strategies. Table 11 represents the system losses and the voltage achieved in the post CM scenario with the application of BFO, GWO, SCA, MRFO, and IMRFO. System losses of 136.63 MW is attained with IMRFO and is minimum when compared to BFO, GWO, SCA, original MRFO. The system voltage attained with the IMRFO has been 0.9786 p.u which is better in comparison to the voltages achieved with BFO, GWO, SCA, and MRFO. The system voltage profiles achieved post CM is represented in Figure 12. Figure 13 characterises the box plot generated from the computation of the congestion costs achieved with SCA, GWO, BFO, MRFO, and IMRFO for 30 trials. The performance of IMRFO is comparatively appreciable than SCA, GWO, BFO, and MRFO. The comparative computational time of SCA, GWO, BFO, MRFO, and IMRFO are represented in Table 12. IMRFO has a computational time of 15.92Sec. and minimum among SCA [solved], GWO [solved], BFO [solved], MRFO [solved]. The comparative convergence mobility analysis based on the convergence rate (CR) has been portrayed in Figure 14. IMRFO has the highest convergence rate as compared to BFO, GWO, SCA, original MRFO.

VI. CONCLUSION

This research work portrayed an effective CM method for the power transmission system. The GSF approach included in this research assisted in the assortment of the sensitive generators that are considered to reschedule their power output. The CM with GSF approach has been beneficial for a higher power system network where the total system generators contributing for the CM can be reduced making the CM strategy robust and economical. The proposed IMRFO with the incorporation of improvement factors has been successful to mitigate the transmission system congestion. Validation of the proposed approach has been done on 39-bus New England system and IEEE 118 bus system.

Comparative performance analysis has been established between the results achieved with IMRFO and the results obtained with RED, ABC,PSO, SCA, BFO, GWO, and MRFO to highlight the effectiveness of IMRFO approach for CM problem. The application of IMRFO has resulted in the reduction of 16.08%, 13.73%, 11.78%, and 4.48 % in congestion when compared to BFO, GWO, SCA, and MRFO for 39-bus New England system. For a larger power system network of 118 bus, the congestion cost reductions have been of 14.84%, 12.97%, 9.63%, and 6.85% when compared to BFO, GWO, SCA, and MRFO. Improvement in the bus voltages and system losses has been observed with IMRFO. Computational time and the convergence rate of IMRFO for the CM problem has been appreciably better than the other applied optimization approach for the CM.

The future scope associated with this work can lead to the investigation of the CM with the influence of Distribution generations and electric vehicles on the distribution side of the power system network. The optimal rescheduling of the thermal generators and the power delivered by the renewable energy sources can be rescheduled to mitigate congestion by enhancing the efficiency of the power system network. Moreover, the analysis of initial operating point (Pg) and the operating point after contingency regarding power flow and voltages can also be analyzed as the extended work in CM.

APPENDIX

See Tables 13 and Table 14.

REFERENCES

[1] H. Hobbie, J. Mehlem, C. Wolff, L. Weber, F. Flachsbarth, D. Möst, and A. Moser, "Impact of model parametrization and formulation on the explorative power of electricity network congestion management models–insights from a grid model comparison experiment," *Renew. Sustain. Energy Rev.*, vol. 159, May 2022, Art. no. 112163.

[2] K. Chakravarthi, P. Bhui, N. K. Sharma, and B. C. Pal, "Real time congestion management using generation re-dispatch: Modeling and controller design," *IEEE Trans. Power Syst.*, early access, Jun. 27, 2022, doi: 10.1109/TPWRS.2022.3186434.

[3] M. Sarwar, A. S. Siddiqui, S. S. M. Ghoneim, K. Mahmoud, and M. M. F. Darwish, "Effective transmission congestion management via optimal DG capacity using hybrid swarm optimization for contemporary power system operations," *IEEE Access*, vol. 10, pp. 71091–71106, 2022.

[4] M. Roustaei, A. Letafat, M. Sheikh, A. Chabok, R. Sadoughi, and M. Ardeshiri, "A cost-effective voltage security constrained congestion management approach for transmission system operation improvement," *Electr. Power Syst. Res.*, vol. 203, Feb. 2022, Art. no. 107674.

[5] V. K. Prajapati and V. Mahajan, "Demand response based congestion management of power system with uncertain renewable resources," *Int. J. Ambient Energy*, vol. 43, no. 1, pp. 103–116, Dec. 2022.

[6] S. J. George, S. K. Ramaraju, V. Venkataraman, T. Kaliannan, U. Kumaravel, and M. Veerasundaram, "Congestion management in deregulated power system by series facts device using heuristic optimization algorithms," *J. Intell. Fuzzy Syst.*, vol. 42, no. 6, pp. 6195–6208, 2022.

[7] D. Singh, N. Pal, S. K. Sinha, and B. Singh, "Allocation of reserved green energy transmission corridors to secure power purchase agreements in smart power networks during congestion management," *Electr. Power Syst. Res.*, vol. 209, Aug. 2022, Art. no. 108006.

[8] A. Narain, S. K. Srivastava, and S. N. Singh, "Congestion management approaches in restructured power system: Key issues and challenges," *Electr. J.*, vol. 33, no. 3, Apr. 2020, Art. no. 106715.

[9] X. Wang, T. Zhao, and A. Parisio, "Frequency regulation and congestion management by virtual storage plants," *Sustain. Energy, Grids Netw.*, vol. 29, Mar. 2022, Art. no. 100586.

[10] W. Zhou, Y. Wang, F. Peng, Y. Liu, H. Sun, and Y. Cong, "Distribution network congestion management considering time sequence of peer-to-peer energy trading," *Int. J. Electr. Power Energy Syst.*, vol. 136, Mar. 2022, Art. no. 107646.

[11] F. U. Haq, P. Bhui, and K. Chakravarthi, "Real time congestion management using plug in electric vehicles (PEV's): A game theoretic approach," *IEEE Access*, vol. 10, pp. 42029–42043, 2022.

[12] F. Shen and Q. Wu, "Robust dynamic tariff method for day-ahead congestion management of distribution networks," *Int. J. Electr. Power Energy Syst.*, vol. 134, Jan. 2022, Art. no. 107366.

[13] S. Voswinkel, J. Höckner, A. Khalid, and C. Weber, "Sharing congestion management costs among system operators using the Shapley value," *Appl. Energy*, vol. 317, Jul. 2022, Art. no. 119039.

[14] J. R. Chintam, "Satin Bowerbird optimization algorithm for the application of optimal power flow of power system with FACTS devices," *Turkish J. Comput. Math. Educ. (TURCOMAT)*, vol. 12, no. 11, pp. 1641–1659, 2021.

[15] J. Srivastava and N. K. Yadav, "Rescheduling-based congestion management by Metaheuristic algorithm: Hybridizing lion and moth search models," *Int. J. Numer. Modelling, Electron. Netw., Devices Fields*, vol. 35, no. 2, Mar. 2022, Art. no. jnm2952.

[16] G. Yesuratnam and D. Thukaram, "Congestion management in open access based on relative electrical distances using voltage stability criteria," *Electr. Power Syst. Res.*, vol. 77, no. 12, pp. 1608–1618, Oct. 2007.

[17] M. EL-Azab, W. A. Omran, S. F. Mekhamer, and H. E. A. Talaat, "Congestion management of power systems by optimizing grid topology and using dynamic thermal rating," *Electr. Power Syst. Res.*, vol. 199, Oct. 2021, Art. no. 107433.

[18] A. Kumar and C. Sekhar, "Comparison of sen transformer and UPFC for congestion management in hybrid electricity markets," *Int. J. Electr. Power Energy Syst.*, vol. 47, pp. 295–304, May 2013.

[19] S. Dutta and S. P. Singh, "Optimal rescheduling of generators for congestion management based on particle swarm optimization," *IEEE Trans. Power Syst.*, vol. 23, no. 4, pp. 1560–1569, Nov. 2008.

[20] J. Hazra, A. K. Sinha, and Y. Phulpin, "Congestion management using generation rescheduling and/or load shedding of sensitive buses," in *Proc. Int. Conf. Power Syst.*, Dec. 2009, pp. 1–5.

[21] A. Agrawal, S. N. Pandey, L. Srivastava, P. Walde, S. Singh, B. Khan, and R. K. Saket, "Hybrid deep neural network-based generation rescheduling for congestion mitigation in spot power market," *IEEE Access*, vol. 10, pp. 29267–29276, 2022.

[22] S. Verma and V. Mukherjee, "Firefly algorithm for congestion management in deregulated environment," *Eng. Sci. Technol., Int. J.*, vol. 19, no. 3, pp. 1254–1265, Sep. 2016.

[23] K. S. Pandya and S. K. Joshi, "Sensitivity and particle swarm optimization-based congestion management," *Electric Power Compon. Syst.*, vol. 41, no. 4, pp. 465–484, Feb. 2013.

[24] F. Zaeim-Kohan, H. Razmi, and H. Doagou-Mojarrad, "Multi-objective transmission congestion management considering demand response programs and generation rescheduling," *Appl. Soft Comput.*, vol. 70, pp. 169–181, Sep. 2018.

[25] S. C. Raja, S. Prakash, and J. J. D. Nesamalar, "Effective power congestion management technique using hybrid Nelder–Mead–grey wolf optimizer (HNMGWO) in deregulated power system," *IETE J. Res.*, 2021, doi: 10.1080/03772063.2021.1963858.

[26] S. Deb and A. K. Goswami, "Congestion management by generator rescheduling using artificial bee colony optimization technique," in *Proc. Annu. IEEE India Conf. (INDICON)*, Dec. 2012, pp. 909–914.

[27] K. Qu, X. Zheng, X. Li, C. Lv, and T. Yu, "Stochastic robust real-time power dispatch with wind uncertainty using difference-of-convexity optimization," *IEEE Trans. Power Syst.*, vol. 37, no. 6, pp. 4497–4511, Nov. 2022.

[28] Y. Welhazi, T. Guesmi, B. M. Alshammari, K. Alqunun, A. Alateeq, Y. Almalaq, R. Alsabhan, and H. H. Abdallah, "A novel hybrid chaotic Jaya and sequential quadratic programming method for robust design of power system stabilizers and static VAR compensator," *Energies*, vol. 15, no. 3, p. 860, Jan. 2022.

[29] C. Li, A. J. Conejo, P. Liu, B. P. Omell, J. D. Siirola, and I. E. Grossmann, "Mixed-integer linear programming models and algorithms for generation and transmission expansion planning of power systems," *Eur. J. Oper. Res.*, vol. 297, no. 3, pp. 1071–1082, Mar. 2022.

[30] A. F. Zobaa, S. A. Aleem, and A. Y. Abdelaziz, *Classical and Recent Aspects of Power System Optimization*. New York, NY, USA: Academic, 2018.

[31] M. Roni, H. Karim, M. Rana, H. Pota, M. Hasan, and M. Hussain, "Recent trends in bio-inspired meta-heuristic optimization techniques in control applications for electrical systems: A review," *Int. J. Dyn. Control*, vol. 10, pp. 999–1011, Jan. 2022.

[32] D. Cekus, P. Kwiatoń, M. Šofer, and P. Šofer, "Application of heuristic methods to the identification of the parameters of discrete-continuous models," *Bull. Polish Acad. Sci., Tech. Sci.*, vol. 70, no. 1, pp. 1–7, 2022.

[33] K. Paul, N. Kumar, S. Agrawal, and K. Paul, "Optimal rescheduling of real power to mitigate congestion using gravitational search algorithm," *Turkish J. Electr. Eng. Comput. Sci.*, vol. 27, no. 3, pp. 2213–2225, 2019.

[34] F. B. Ozsoydan and A. Baykasoglu, "Analysing the effects of various switching probability characteristics in flower pollination algorithm for solving unconstrained function minimization problems," *Neural Comput. Appl.*, vol. 31, no. 11, pp. 7805–7819, Nov. 2019.

[35] K. Paul and N. Kumar, "Cuckoo search algorithm for congestion alleviation with incorporation of wind farm," *Int. J. Electr. Comput. Eng. (IJECE)*, vol. 8, no. 6, p. 4871, Dec. 2018.

[36] K. Paul, P. Sinha, S. Mobayen, F. F. M. El-Sousy, and A. Fekih, "A novel improved crow search algorithm to alleviate congestion in power system transmission lines," *Energy Rep.*, vol. 8, 2022, doi: 10.1016/j.egyr.2022.08.267.

[37] W. Zhao, Z. Zhang, and L. Wang, "Manta ray foraging optimization: An effective bio-inspired optimizer for engineering applications," *Eng. Appl. Artif. Intell.*, vol. 87, Jan. 2020, Art. no. 103300.

[38] M. Abd Elaziz, D. Yousri, M. A. A. Al-qaness, A. M. Abdelaty, A. G. Radwan, and A. A. Ewees, "A Grunwald–Letnikov based manta ray foraging optimizer for global optimization and image segmentation," *Eng. Appl. Artif. Intell.*, vol. 98, Feb. 2021, Art. no. 104105.

[39] K. K. Ghosh, R. Guha, S. K. Bera, N. Kumar, and R. Sarkar, "S-shaped versus V-shaped transfer functions for binary manta ray foraging optimization in feature selection problem," *Neural Comput. Appl.*, vol. 33, no. 17, pp. 11027–11041, Jan. 2021.

[40] H. Xu, H. Song, C. Xu, X. Wu, and N. Yousefi, "Exergy analysis and optimization of a HT-PEMFC using developed manta ray foraging optimization algorithm," *Int. J. Hydrogen Energy*, vol. 45, no. 55, pp. 30932–30941, Nov. 2020.

[41] M. G. Hemeida, A. A. Ibrahim, A.-A.-A. Mohamed, S. Alkhalaf, and A. M. B. El-Dine, "Optimal allocation of distributed generators DG based manta ray foraging optimization algorithm (MRFO)," *Ain Shams Eng. J.*, vol. 12, no. 1, pp. 609–619, Mar. 2021.
[42] A. Fathy, H. Rezk, and D. Yousri, "A robust global MPPT to mitigate partial shading of triple-junction solar cell-based system using manta ray foraging optimization algorithm," *Sol. Energy*, vol. 207, pp. 305–316, Sep. 2020.
[43] S. Mirjalili, S. M. Mirjalili, and A. Lewis, "Grey wolf optimizer," *Adv. Eng. Softw.*, vol. 69, pp. 46–61, Mar. 2014.
[44] C. Li, Z. Luo, Z. Song, F. Yang, J. Fan, and P. X. Liu, "An enhanced brain storm sine cosine algorithm for global optimization problems," *IEEE Access*, vol. 7, pp. 28211–28229, 2019.
[45] S. Das, A. Biswas, S. Dasgupta, and A. Abraham, "Bacterial foraging optimization algorithm: Theoretical foundations, analysis, and applications," in *Foundations of Computational Intelligence*, vol. 3. Cham, Switzerland: Springer, 2009, pp. 23–55.
[46] K. Padiyar, *Power System Dynamics: Stability & Control*. Hyderabad, India: BS Publications, 2010.
[47] S. Sivakumar and D. Devaraj, "Congestion management in deregulated power system by rescheduling of generators using genetic algorithm," in *Proc. Int. Conf. Power Signals Control Computations (EPSCICON)*, Jan. 2014, pp. 1–5. [Online]. Available: https://ieeexplore.ieee.org/document/6887495
[48] M. Sarwar, A. S. Siddiqui, Z. A. Jaffery, and D. P. Kothari, "Bid responsive generation rescheduling for congestion management in electricity market," *Eng. Rep.*, vol. 3, no. 5, May 2021, Art. no. e12331.

KAUSHIK PAUL received the Ph.D. degree from the NIT Jamshedpur with specialization in power system, and the M.Tech. degree in demand response and designing of smart meters for residential energy consumption from the NIT Kurukshetra. He is currently working as an Assistant Professor with the Department of Electrical Engineering, BIT Sindri. He has published papers in the field of optimization techniques application for optimal power system operations and also working on the application of machine learning approaches for enhancement of power system operations. His research interests include power system congestion management, application of optimization of techniques for optimal system operation, renewable energy integration, and demand side management.

PAMPA SINHA received the Ph.D. degree in electrical engineering from Jadavpur University, West Bengal, India. She is currently working as an Assistant Professor with KIIT Deemed to be University, Bhubaneswar, India. Her research interests include power quality monitoring, energy management, and harmonic analysis. Her conference papers awarded as the best paper award.

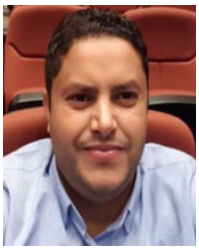

YASSINE BOUTERAA received the National Engineering degree in electrical engineering from the National School of Engineers of Sfax, in June 2006, the Master of Science degree in control and computer science, in 2007, the Ph.D. degree in electrical and computer engineering from the University of Orleans, France, and the University of Sfax, in 2012, and the HDR degree (accreditation to supervise research) in electrical and computer engineering, in 2017. He is the author/coauthor of more than 50 scientific articles. His research interests include robotics, embedded systems, and real time implementation. He is a reviewer of some indexed journals and a TPC member of some international conferences.

PAWEŁ SKRUCH (Senior Member, IEEE) received the M.S. degree (Hons.) in automation control and the Ph.D. degree (summa cum laude) from the Faculty of Electrical Engineering, Automatics, Computer Science and Electronics, and the D.Sc. (Habilitation) degree in automatics and robotics from the AGH University of Science and Technology, Krakow, Poland, in 2001, 2005, and 2016, respectively. He is currently a Professor of control engineering with the AGH University of Science and Technology and also an Advanced Engineering Manager of AI and safety with the Aptiv Technical Center, Krakow. His current research interests include dynamical systems, autonomous systems, artificial intelligence, machine learning, modeling and simulation, and applications of control theory to software systems.

SALEH MOBAYEN (Senior Member, IEEE) was born in Khoy, Iran, in 1984. He received the B.Sc. and M.Sc. degrees in electrical engineering from the Department of Control Engineering, University of Tabriz, Tabriz, Iran, in 2007 and 2009, respectively, and the Ph.D. degree in electrical engineering from the Department of Control Engineering, Tarbiat Modares University, Tehran, Iran, in January 2013. From January 2013 to December 2018, he was an Assistant Professor and a Faculty Member with the Department of Electrical Engineering, University of Zanjan, Zanjan, Iran, where he has been an Associate Professor of control engineering, since December 2018. From July 2019 to September 2019, he was a Visiting Professor at the University of the West of England (UWE), Bristol, U.K., with financial support from the Engineering Modeling and Simulation Research Group, Department of Engineering Design and Mathematics. Since 2020, he has been an Associate Professor with the National Yunlin University of Science and Technology (YunTech), Taiwan, and collaborated with the Future Technology Research Center (FTRC). He has published several papers in the national and international journals. His research interests include control theory, sliding mode control, robust tracking, non-holonomic robots, and chaotic systems. He is a member of the IEEE Control Systems Society and serves as a member of program committee of several international conferences. He is an Associate Editor of several international scientific journals and has acted as a symposium/track co-chair in numerous IEEE flagship conferences. He is a world's top 2% scientist from Stanford University (from 2019 until now), and has been ranked among 1% top scientists in the world in the broad field of electronics and electrical engineering. He is also recognized in the list of top electronics and electrical engineering scientists in Iran.